Computers and Concrete, *Vol. 17, No. 2 (2016) 281-294*
DOI: http://dx.doi.org/10.12989/cac.2016.17.2.281

Effect of fiber geometry on the electromagnetic shielding performance of mortar

Young Jun Kim, Dinberu M. Yemam, Baek-Joong Kim and Chongku Yi*

School of Civil, Environmental and Architectural Engineering, Korea University
145 Anam-ro, Seongbuk-gu, Seoul 02841, Republic of Korea

(Received October 30, 2015, Revised November 28, 2015, Accepted December 3, 2015)

Abstract. The increased awareness of electromagnetic wave hazards has prompted studies on electromagnetic shielding using conductive materials in the construction industry. Previous studies have explored the effects of the types of conductive materials and their mix proportions on the electromagnetic shielding performance; however, there has been insufficient research on the effect of the geometry of the conductive materials on the electromagnetic shielding performance. Therefore, in this study, the dependence of the electromagnetic shielding performance on the cross-sectional geometry, diameter and length of fibers was investigated. The results showed that the electromagnetic shielding performance improved when the fiber length increased or the diameter decreased, but the effect of the cross-sectional geometry of the fibers was smaller than the effect of the fiber spacing factor.

Keywords: electromagnetic wave; shielding effectiveness; metal fiber; geometry; spacing factor

1. Introduction

Electromagnetic waves, which are composed of electric and magnetic fields acting at right angles, can be generated for purpose of long-distance electrical transmission or produced during normal operation of electronic equipment. Exposure to electromagnetic waves has been reported to affect human health (Genuis 2008, Greenland *et al.* 2000, Kabuto *et al.* 2006). Li *et al.* (2002) reported that the risk of miscarriage increased up to 1.8 times when the amount of exposure to electromagnetic waves during pregnancy was more than 16 mG. Draper *et al.* (2005) also stated the relative risk (RR) of leukemia was 70% higher in areas within 200 m of a high-voltage power line than in areas that are 600 m away. In addition, the electromagnetic waves can interfere with electronic signals inducing equipment malfunction or failure (Min 2009). Especially, the electromagnetic interference (EMI) technology for military application is a risk for national security. A typical example is an electromagnetic pulse bomb that can disable social civil and military systems by disabling communication and electronic devices.

Studies on electromagnetic shielding have been conducted to protect important building

*Corresponding author, Professor, E-mail: chongku@korea.ac.kr

http://www.techno-press.org/?journal=cac&subpage=8 ISSN: 1598-8198 (Print), 1598-818X (Online)

structures or humans from electromagnetic wave hazards. In some of these studies conductive materials were used for electromagnetic shielding because of their property to reflect or absorb electromagnetic waves (White and Mardiguian 1988). Lee *et al.* (2003) applied carbon-based paint-like conductive materials on a wall and measured an electromagnetic shielding effectiveness of 9 dB in the frequency range of 30-1.5 GHz. Suchea *et al.* (2015) applied a paint-like material containing graphene, Cu particles, and multi-walled carbon nanotubes (MWCNT) on a foam board and reported an electromagnetic shielding effectiveness of 20-30 dB in the frequency range of 30-1.5 GHz. However, paint-like shielding materials tend to get scratched easily, thus resulting in low durability and increased maintenance cost. Hence, other studies have taken a different direction by mixing conductive materials with other materials such as cementitious composite (Guan *et al.* 2006). Especially, carbon-based materials have been used in many previous studies due to their relatively high electrical conductivity. Chiou *et al.* (1989) found that a cement paste containing 4 wt.% carbon fiber had a shielding performance of up to 25 dB. Kim *et al.* (2006) reported that epoxy composite containing 1.6 wt.% carbon black had a shielding effectiveness of approximately 40 dB at a frequency of 850 MHz. Micheli *et al.* (2014) reported that a cement composite containing carbon nanotube (CNT) had a high shielding effectiveness of approximately 50 dB in the frequency range of 0.75-1.12 GHz.1 Although these carbon-based materials have high electromagnetic shielding effectiveness, their practical application is economically infeasible due to high costs. Thus, electromagnetic shielding studies using metal fibers, which have a relatively low manufacturing cost and good conductivity, have also been undertaken. Wen and Chung (2004) reported that a cement paste containing steel fibers with 8-μm diameter had an electromagnetic shielding effectiveness of up to 70 dB. Shyr and Shie (2012) produced a textile containing stainless steel fibers and observed its shielding effectiveness to be more than 50 dB in the frequency range of 30-1,500 MHz. Recently, as the interest in environmental protection has grown, studies on the electromagnetic shielding performance of conductive industrial by-products have also been undertaken (Bantsis *et al.* 2012, Baoyi *et al.* 2012, Kim and Yi 2015, Lim *et al.* 2011). These studies showed that the electromagnetic shielding performance of the conductive industrial by-products was similar to that of previously studied conductive materials, but the possible deterioration of the mechanical properties of cement composites containing industrial by-products may have limited their practical application (Albano *et al.* 2005, Eisa 2014, Ghernouti and Rabehi 2012, Khatib and Bayomy 1999).

These existing studies have shown that the inclusion of electrically conductive materials in a composite matrix can improve the electromagnetic shielding performance of the composite material. However, the findings were limited to the electromagnetic shielding performance with respect to different types or mix proportions of the conductive materials. The electromagnetic shielding performance of cement composites with regard to the geometry of the conductive material, thus far, has not been studied.

In this study, the effect of fiber geometry on electromagnetic shielding performance of fiber-reinforced mortar was first evaluated experimentally, and the significances of the fiber length, diameter, and volume fraction on electromagnetic shielding performance were further discussed based on a regression analysis.

2. Experiment

Experiments were carried out to determine the effects of fiber geometry on the electromagnetic

Table 1 Mineral composition of cement (by wt.%)

C_3S	C_2S	C_3A	C_4AF	Gypsum
51.87	19.42	4.84	10.27	3.90

Table 2 Chemical composition of cement (by wt.%)

CaO	SiO_2	Al_2O_3	MgO	Fe_2O_3	SO_3
58.6	22.1	6.4	4.1	3.5	2.6
K_2O	TiO_2	P_2O_5	Na_2O	Ig. loss	
1.8	0.3	0.3	0.2	0.2	

Table 3 Properties of metal fibers

Metal fiber	Stainless Steel Fiber(SSF)	Amorphous Steel Fiber(ASF)	High Carbon Steel Fiber(HCF)
Cross section (mm)	Circle ϕ 0.2, 0.3, 0.4	Rectangle 1.6×0.029	Triangle 0.57×0.57×0.57
Length (mm)	12, 16, 20, 24, 28	20	10, 20
Composition (wt.%)	Fe(73), Cr(18), Ni(8)	Fe(79), Cr(7)	Fe(94), C(0.6), Ni(5)

shielding performance of fiber-reinforced mortars according to ASTM D 4935 and KS C 0304.

2.1 Materials

Ordinary Portland cement (type 1 per KS L 5201) with a density of 3.11 g/cm^3 and sand with a density of 2.62 g/cm^3 and absorption of 1.62% were used for preparing the mortar. Tables 1 and 2 summarize the chemical and mineral compositions of the cement.

Three different types of metal fiber reinforcements with different geometries (SSF, ASF and HCF) were used as conductive shielding materials for inclusion in the mortar. SSF fibers of various diameters and lengths were also used to examine the effects of the length and diameter of the fibers on their electromagnetic shielding performance. The properties and main compositions of the metal fibers are shown in Table 3.

Fig. 1 shows the geometries of the metal fibers. SSF and ASF have circular and thin rectangular cross sections, respectively, while HCF is a twisted fiber that has a triangular cross section. The twisted surface of HCF gives the fiber various reflection angles when it encounters

(a) SSF (b) ASF (c) HCF

Fig. 1 Image of metal fibers

Table 4 Specimens considered in this study

Type		Metal fiber		Volume fraction (vol.%)
		Diameter (mm)	Length (mm)	
SSF	S_2_12	0.2	12	0, 0.3, 0.5
	S_2_16	0.2	16	
	S_2_20	0.2	20	
	S_2_24	0.2	24	
	S_2_28	0.2	28	
	S_3_12	0.3	12	
	S_3_16	0.3	16	
	S_3_20	0.3	20	
	S_3_24	0.3	24	
	S_3_28	0.3	28	
	S_4_12	0.4	12	
	S_4_16	0.4	16	
	S_4_20	0.4	20	
	S_4_24	0.4	24	
	S_4_28	0.4	28	
ASF	A_20	1.6×0.029	20	
HCF	H_10	0.57×0.57×0.57	10	
	H_20	0.57×0.57×0.57	20	

waves, but SSF and ASF fibers have untwisted surfaces resulting in constant reflection angles.

2.2 Mix proportions

Mortars having a cement-to-fine-aggregate ratio of 1:2 and a water-to-binder ratio of 0.4 were prepared for control specimens, and SSF-, ASF- and HCF-fiber-reinforced mortars at two volume fractions of 0.3 % and 0.5 % were then prepared. The mix proportions of the mortars studied are given in Table 4.

2.3 Test method

Test specimens were prepared as per ASTM D 4935. First, dry mixing of cement, sand, and metal fiber was performed for 30 s to ensure a uniform distribution of the fiber in the mixture using a mixer. Then, water was added and wet mixing was continued for 1 min and 30 s. The prepared mixture was then poured into a plastic mold and compacted using a vibrating table. After casting, the specimens were sealed and stored at 25±1°C and 50±2% relative humidity for 24 h. The specimens were then demolded and cured in water at 23±3°C. For each mix proportion, one test and one reference specimen were cast and cured. On the 7th day of curing, the test and reference specimens were sliced and polished, to prepare three samples and one sample, respectively, with a thickness of 5 mm. The surfaces of the samples were polished to minimize

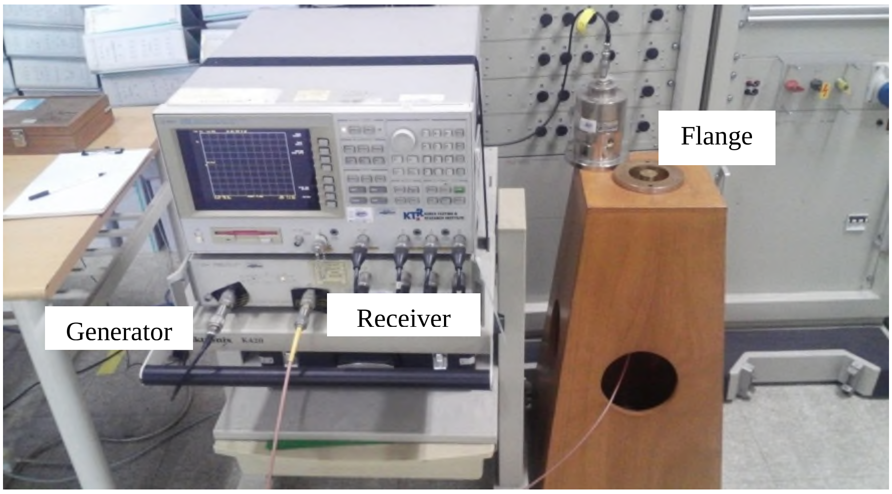

Fig. 2 Image of the experimental set-up

scattering of the electromagnetic waves when they were applied to the surface of the sample. The thickness of the specimen was set to 5 mm to fulfill the requirements of ASTM D 4935 as well as KS C 0304, which limits the thickness of a specimen to less than or equal to 5 mm (KSA 2014).

The electromagnetic shielding performance of the mortars was measured by using a flanged coaxial transmission guide setup as stated in ASTMInternational (2010), which covers a broad range of wave frequencies from 300 MHz to 1.5 GHz. The test samples were first placed between the two flanges, then electromagnetic waves produced by the signal generator were applied on one side of the samples and the power received on the other side of the flange was measured by the signal receiver. These measured powers were later used to compute the electromagnetic shielding effectiveness of the test specimens. Fig. 2 shows the equipment used to perform this experiment.

2.4 Related equations

The electromagnetic shielding effectiveness (SE) is obtained according to Eq. (1) as shown below. The received power without the sample present (P_2) was measured by placing a reference specimen that has an open region to allow free transmission of electromagnetic waves, and the received power with the sample present (P_1) was measured by placing the test specimen. Fig. 3 shows the reference and test specimen.

$$SE = -10\log\frac{P_1}{P_2} \text{ (dB)} \tag{1}$$

where, P_1 : received power with the material present (W) and

P_2 : received power without the material present (W)

It is noted that the shielding effectiveness value, being expressed in decibel, allows to see the minute changes in the performance of a material, but also may mislead interpretation of the results as log scale is not as common as linear scale. For example, materials, having only 1 % difference in electromagnetic power loss (90% and 99%), can have two folds difference in terms of SE values

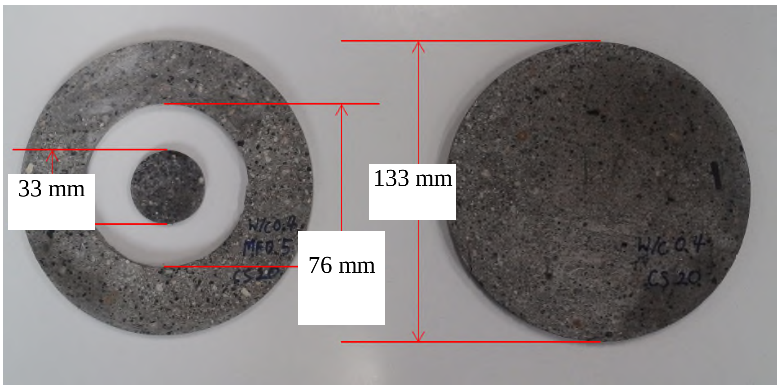

(a) Reference (b) Test

Fig. 3 Image of a typical pair of specimens

(10 dB and 20 dB). Furthermore, extra care is required to carry out arithmetic operation on SE values to analyze the data. Hence, in this study, shielding rate (%), per Eq. (2), was adapted to compare and discuss the experimental results.

$$Shielding\ rate = \frac{P_1}{P_2} \times 100\ (\%) \tag{2}$$

where, P_1 : received power with the material present and

P_2 : received power without the material present

It is well known that the effect of fiber reinforcement on the mechanical properties of mortar is closely related to the ways that the fibers are distributed in the matrix. In an attempt to quantify the effectiveness of fibers, the notion of fiber spacing factor has been introduced. The formula for the fiber spacing factor, Eq. (3), was suggested by James *et al.* in 1964 with the assumption that the fibers are evenly distributed (James and James 1964).

$$S = 13.8d\sqrt{\frac{1}{V_f}} \tag{3}$$

where, S : Fiber spacing factor,

V_f : Fiber volume fraction (vol.%)

d : Diameter of fiber (mm)

3. Results and discussion

Figs. 4-5 presents the shielding effectiveness (SE) vs. frequency results obtained from mortars reinforced with SSF having three different diameters, five different lengths, and two different fiber volume fractions. Each graph shows that the shielding effectiveness was affected by the fiber diameter for a given length and volume fraction, and the improvement in the shielding

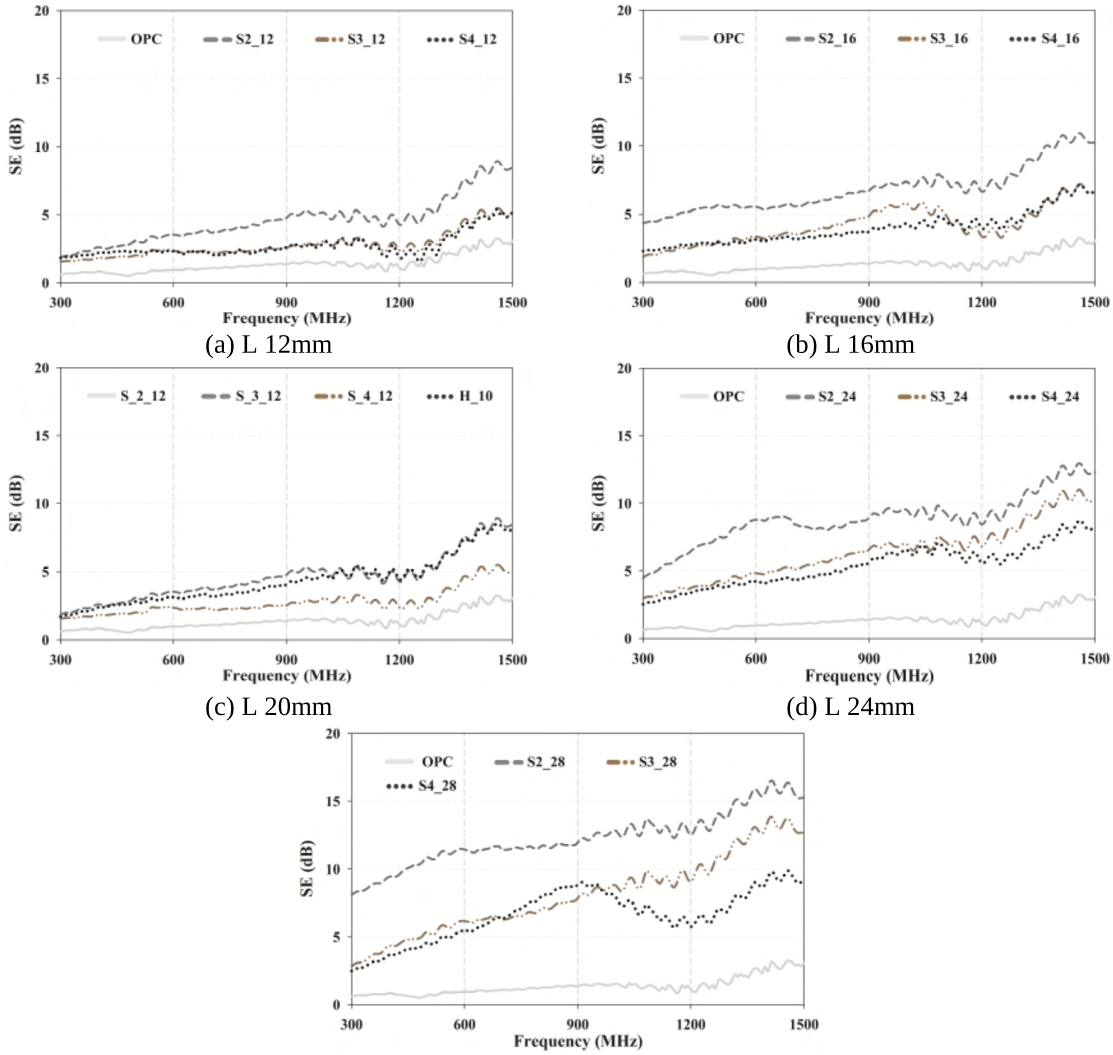

(a) L 12mm

(b) L 16mm

(c) L 20mm

(d) L 24mm

(e) L 28mm

Fig. 4 Shielding effectiveness of mortar (SSF, V_f 0.3%)

performance of mortars reinforced with fiber can be easily appreciated by comparing the graphs of the fiber-reinforced mortars with the one for the control specimen (OPC). These results also clearly showed that the shielding effectiveness increased with the wave frequency. In particular, when the frequency was more than 1,200 MHz, the increase in shielding effectiveness was more distinct. This may arise from the tendency of electromagnetic waves to easily diffract at low frequencies, but not so easily at high frequencies.

3.1 Effect of fiber size on shielding performance

Fig. 6 shows the improved electromagnetic shielding rate of SSF-reinforced mortar over OPC, averaged over the frequency range of 300–1500 MHz for three different diameters and five

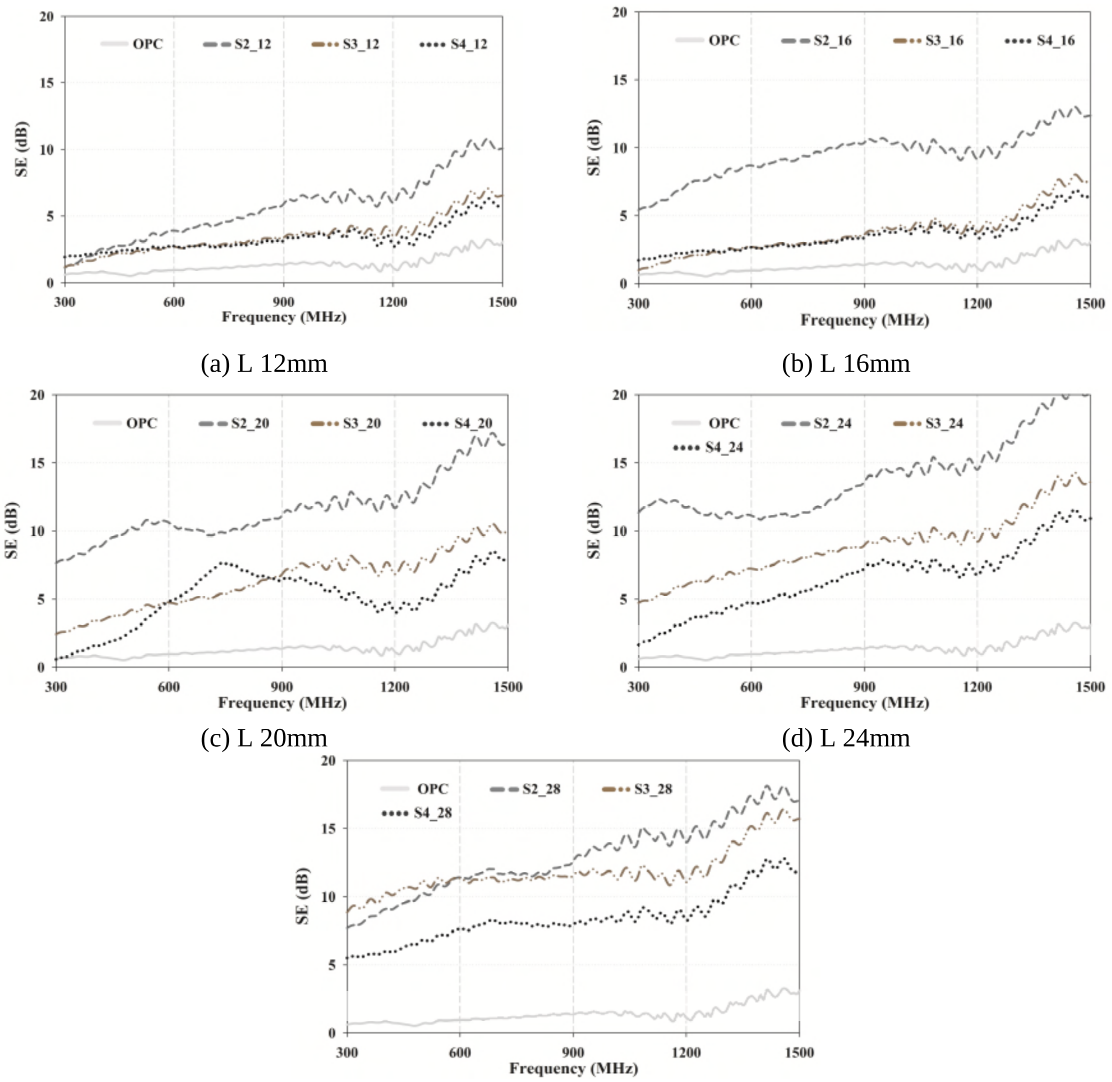

(a) L 12mm

(b) L 16mm

(c) L 20mm

(d) L 24mm

(e) L 28mm

Fig. 5 Shielding effectiveness of mortar (SSF, V_f 0.5%)

different lengths of SSF. The results showed that the minimum improvement in shielding rate of SSF reinforced mortar was nearly 20%. The average enhancements in shielding rates for the five fiber lengths were 35.7% for 0.4 mm fiber diameter, 39.8% for 0.3 mm, and 53.6% for 0.2 mm, respectively, at a volume fraction of 0.3%.

The same trend was observed at a volume fraction of 0.5%; where the average enhancements in shielding rates for the five fiber lengths were 39.8% 45.1%, 61.2% for 0.4 mm, 0.3 mm, and 0.2 mm fiber diameter, respectively. These results suggest that the electromagnetic shielding rate of the mortar improves as the fiber diameter decreases. The results can be attributed to a denser distribution of fibers in the matrix due to the increase in the number of fibers with smaller diameters for a given length and volume fraction.

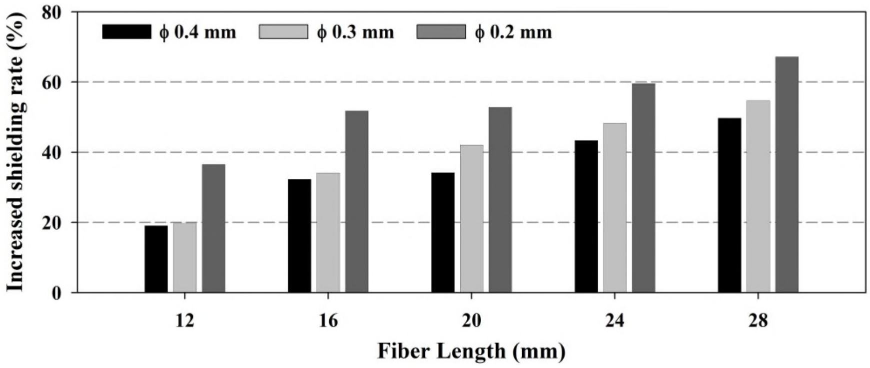

(a) Volume fraction 0.3 %

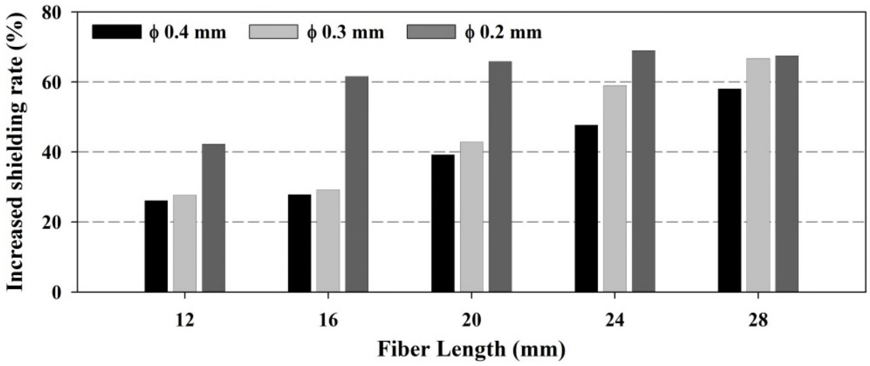

(b) Volume fraction 0.5 %

Fig. 6 Increase in the average electromagnetic shielding compared to that of OPC (%)

Fig. 6 shows the relationship between the improved electromagnetic shielding rates of SSF-reinforced mortar vs. SSF fiber length. The improved electromagnetic shielding rate increased with the length of the fiber. At the V_f of 0.3%, the average enhancements in electromagnetic shielding rates for the three fiber diameters were 27.8%, 39.4%, 43.0%, 50.3%, and 57.2% for the fiber length of 12 mm, 16 mm, 20 mm, 24 mm, and 28 mm, respectively. At the V_f of 0.5%, the average enhancements in electromagnetic shielding rates for the three fiber diameters were 32.0%39.6%, 51.0%, 58.6%, and 64.1% for a fiber length of 12 mm, 16 mm, 20 mm, 24 mm, and 28 mm, respectively. However, at the V_f of 0.5%, the improved electromagnetic shielding rate for 0.2-mm diameter fibers having 24 mm and 28 mm lengths was found to decrease from 69.0% to 67.5%, respectively. This trend is opposite to the other results where the increase in electromagnetic shielding rate showed a positive relation with the fiber length. This can be attributed to the fiber ball effect that can result in an uneven distribution of fibers in the matrix, which was clearly observed during mixing of fibers with 0.2-mm diameter and 28-mm length.

3.2 Effect of spacing factor on shielding performance

Fig. 7 shows the shielding rate, averaged over the frequency range of 300-1500 MHz, with respect to the spacing factors. The spacing factor varied depending on the volume fraction and fiber diameter. For a fiber diameter of 0.2 mm and a volume fraction of 0.5%, the spacing factor

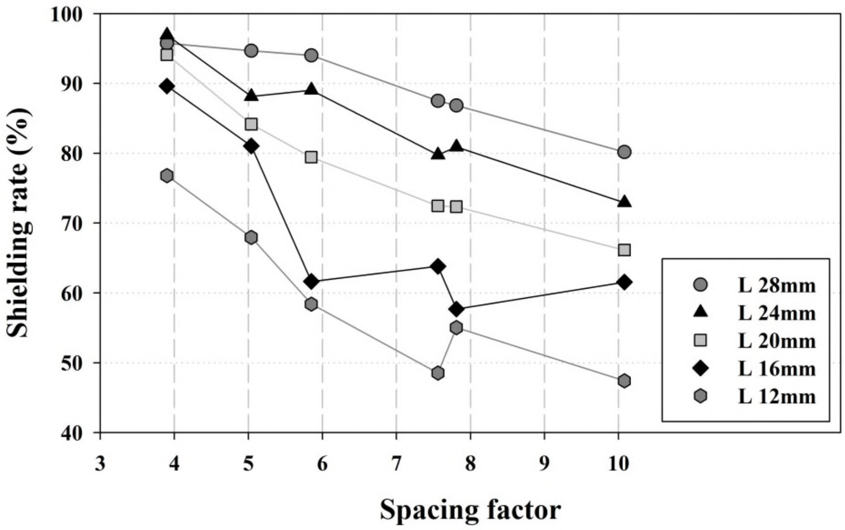

Fig. 7 SE versus Spacing factor

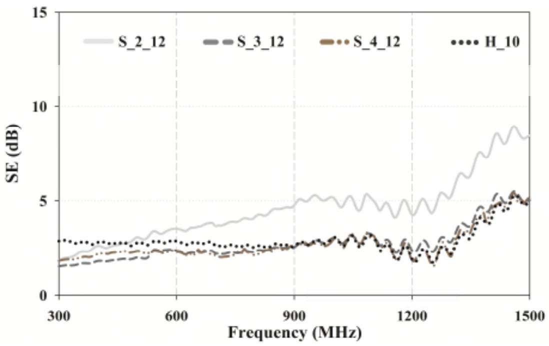

(a) Length 10 mm / V_f 0.3 vol.%

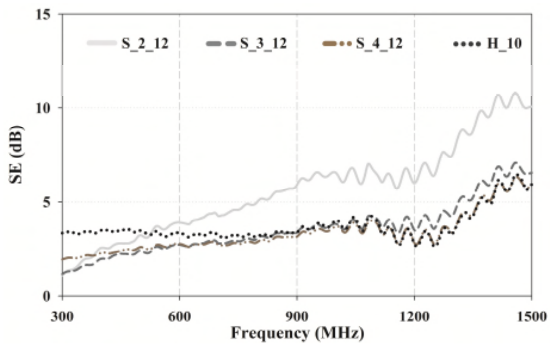

(b) Length 10 mm / V_f 0.5 vol.%

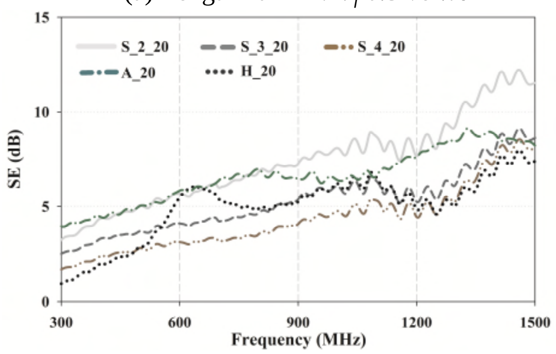

(c) Length 20 mm / V_f 0.3 vol.%

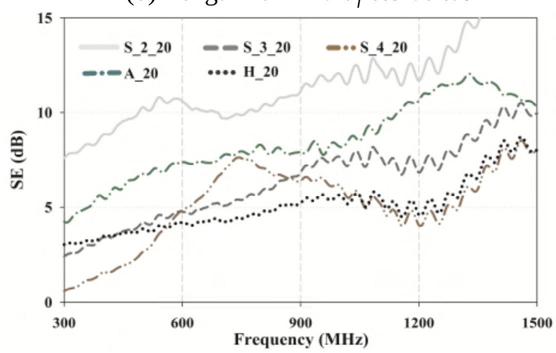

(d) Length 20 mm / V_f 0.5 vol.%

Fig. 8 Effect of cross-section shape on SE

was at its minimum value of 3.9, and for a fiber diameter of 0.4 mm and a volume fraction of 0.3%, the spacing factor was at its maximum value of 10.08. The results suggest that the

Table 5 Equivalent diameter of non-circular fibers

Steel fiber	SSF 0.2 mm	ASF	SSF 0.3 mm	SSF 0.4 mm	HCF
Cross-section area (mm^2)	0.031	0.046	0.071	0.126	0.143
Diameter (mm)	0.2	0.24	0.3	0.4	0.43

electromagnetic shielding rate increases as the spacing factor decreases. This indicates that the shielding effectiveness increases as the distance between fibers become smaller, resulting in a denser distribution of fiber in the matrix. In addition, the shielding rate vs. spacing factor graphs tend to fluctuate for the fiber lengths of 12 mm and 16 mm, while they show a more linear trend for longer fibers.

3.3 Effect of fiber cross-section geometry on SE

The graph in Fig. 8 shows the results obtained from mortars reinforced with three types of fibers having three different geometries (SSF, ASF and HCF). The fibers used also varied in length, diameter, or volume fraction. The shielding effectiveness of HCF-reinforced mortars showed a very similar trend with 0.4-mm SSF diameter in the high-frequency region, while in the low-frequency region they showed relatively higher values for a given fiber length and volume fraction. For the ASF specimens, the shielding effectiveness values were found to be lower than for SSF with 0.2-mm diameter and higher than for SSF with 0.3-mm diameter.

However, the three types of fibers have different cross-sectional areas as well as cross-sectional geometry. Thus, simple comparison of the electromagnetic shielding performance of these fibers based on the above graphs is difficult. Therefore, in this study, the spacing factor was used to analyze the effect of cross-sectional geometry on the electromagnetic shielding performance. The fiber spacing factors were calculated using the diameter and volume fractions of fibers. In the case of non-circular fibers (HCF and ASF), the equivalent diameters were adopted for the calculation (Choi et al. 2012). Table 5 summarizes the diameters of fibers while length is 10 mm for HCF, 12 mm for SSF, and 20 mm for SSF, ASF, and HCF. The equivalent diameter of ASF was found to be between the 0.2-mm and 0.3-mm diameters of SSF, while the equivalent diameter of HCF was found to slightly higher than the 0.4-mm diameter of SSF.

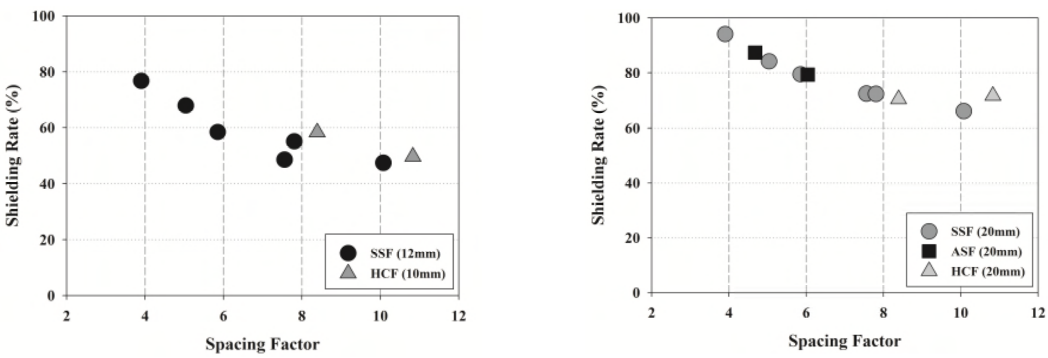

(a) Length 10, 12 mm (b) Length 20 mm

Fig. 9 Effect of fiber cross-section geometry on SE

Fig. 9 shows the relationship between spacing factors and average electromagnetic shielding rates of the metal fibers with different cross-sectional geometries. An inverse relationship between the spacing factor and the electromagnetic shielding rates regardless of the length of the fiber was evident.

3.4 Regression analysis

To analyze the relative influence of the factors affecting the electromagnetic shielding performance of the fiber-containing mortar, the electromagnetic shielding rate (%) averaged over the frequency range of 300-1,500 MHz was the dependent variable, and the length, diameter, and volume fractions of the fibers were considered as the independent variables. The equation for the shielding rate found by the regression analysis, using SPSS, is as follows.

$$F = 53.700 + 1.929X_1 - 94.500X_2 + 30.667X_3 > 0,\ R^2 = 0.913 \quad (4)$$

Where F is the average electromagnetic shielding rate of the mortar (%), X_1 is the length of the fiber (mm), X_2 is the diameter of the fiber (mm), and X_3 is the volume fraction of the fiber (vol.%). The result of the analysis showed that the electromagnetic shielding performance of the mortar was proportional to the fiber length and volume fraction and was inversely proportional to the fiber diameter. Eq. (4) indicates that the average electromagnetic shielding rate increases by 1.929% when the fiber length increases by 1 mm, and the average electromagnetic shielding rate increases by 9.45% when the fiber diameter decreases by 0.1 mm. Also, the average electromagnetic shielding rate increases by 3.067% when the volume fraction increases by 0.1%.

In order to analyze the relation between dependent variable and each independent variable considered in this study, the variables were transformed into standard form (Michael 1997), where independent variables are standardized by their coefficients. In this study, the standardized coefficient values of the independent variables were found to be 0.760 for X_1, -0.538 for X_2, and 0.214 for X_3. The analysis results, therefore, suggest that fiber length had the largest effect on the electromagnetic shielding rate of the mortar and volume fraction had the least effect on the electromagnetic shielding rate.

4. Conclusions

In this study, the following conclusions were obtained based on the results of the experiments.

(1) The electromagnetic shielding performance of the mortar compared to OPC was improved by 1.7-3.5 times at a volume fraction of 0.3% and by 2.0-3.6 times at a volume fraction of 0.5%.

(2) The electromagnetic shielding performance of the fiber-reinforced mortar improved when the diameter of the mixed fibers decreased or the fiber length increased for a given volume fraction of fiber. Moreover, for a given fiber diameter and length, the electromagnetic shielding performance improved when the fiber volume fraction increased.

(3) In this study, the effect of the fiber cross-sectional geometry on the electromagnetic shielding effectiveness of the mortar was not distinct, but a strong relation between the electromagnetic shielding rate and the fiber spacing factor was observed.

(4) Regression analysis results showed that the fiber length had the largest effect on the electromagnetic shielding performance, and the fiber volume fraction had the smallest effect.

Through this study, the trends of electromagnetic shielding with the geometry and size of the fibers (diameter, length, and cross-sectional geometry) were investigated. Fibers having smaller diameters, greater lengths, are recommended for a high electromagnetic shielding effectiveness. However, the fiber length should be small enough to avoid forming fiber balls. Based on the results of this study, shielding experiment using concrete and polymers are planned for the future; by these efforts, it is anticipated that construction materials for electromagnetic shielding that can be used in various environments will be developed.

Acknowledgements

This research was supported by Basic Science Research Program through the National Research Foundation of Korea (NRF) funded by the Ministry of Education, Science and Technology (NRF-2013R1A1A2012788). In addition, in part, this work was supported by the New & Renewable Energy Core Technology Program of the Korea Institute of Energy Technology Evaluation and Planning(KETEP) granted financial resource from the Ministry of Trade, Industry & Energy, Republic of Korea (No. 2013030020820)

References

Albano, C., Camacho, N., Reyes, J., Feliu, J.L. and Hernández, M. (2005), "Influence of scrap rubber addition to Portland I concrete composites: destructive and non-destructive testing", *Comp. Struct.*, **71**(3), 439-446.

ASTM International (2010), *Standard test method for measuring the electromagnetic shielding effectiveness of planar materials*, Americal Society of Testing Materials, America.

Bantsis, G., Mavridou, S., Sikalidis, C., Betsiou, M., Oikonomou, N. and Yioultsis, T. (2012), "Comparison of low cost shielding-absorbing cement paste building materials in X-band frequency range using a variety of wastes", *Ceram. Int.*, **38**(5), 3683-3692.

Baoyi, L., Yuping, D. and Shunhua, L. (2012), "The electromagnetic characteristics of fly ash and absorbing properties of cement-based composites using fly ash as cement replacement", *Constr. Build. Mater.*, **27**(1), 184-188.

Chiou, J.M., Zheng, Q. and Chung, D.D.L. (1989), "Electromagnetic interference shielding by carbon fibre reinforced cement", *Composites*, **20**(4), 379-381.

Choi, H.J. and Choi, K.K. (2012), "A prediction model of shrinkage cracking of steel fiber reinforced concrete", *J. Architec. Inst. Korea Struct. Constr.*, **28**(6), 59-66.

Draper, G. and Vincent, T. (2005), "Childhood cancer in relation to distance from high voltage power lines in England and Wales: a case-control study", **330**(7503), 1290.

Eisa, A. (2014), "Properties of concrete incorporating recycled post-consumer environmental wastes", *Int. J. Concrete Struct. Mater.*, **8**(3), 251-258.

Genuis, S.J. (2008), "Fielding a current idea: exploring the public health impact of electromagnetic radiation", *Public Health*, **122**(2), 113-124.

Ghernouti, Y. and Rabehi, B. (2012), "Strength and durability of mortar made with plastics bag waste (MPBW)", *Int. J. Concrete Struct. Mater.*, **6**(3), 145-153.

Greenland, S. and Sheppard, A.R. (2000), "A pooled analysis of magnetic fields, wire codes, and childhood leukemia", *Epidemiology*, **11**(6), 624-634.

Guan, H., Liu, S., Duan, Y. and Cheng, J. (2006), "Cement based electromagnetic shielding and absorbing building materials", *Cement Concrete Comp.*, **28**(5), 468-474.

James, P.R. and James, A.M. (1964), “Tensile strength of concrete affected by uniformly distributed and closely spaced short lengths of wire reinforcement”, *J. Proc.*, **61**(6), 657-672.

Kabuto, M. and Nitta, H. (2006), “Childhood leukemia and magnetic fields in Japan: A case-control study of childhood leukemia and residential power-frequency magnetic fields in Japan”, *Int. J. Cancer*, **119**(3), 643-650.

Kabuto, M., Nitta, H., Yamamoto, S., Yamaguchi, N., Akiba, S., Honda, Y. and Nakamura, Y. (2006), “Childhood leukemia and magnetic fields in Japan: A case-control study of childhood leukemia and residential power-frequency magnetic fields in Japan”, *Int. J. Cancer*, **119**(3), 643-650.

Khatib, Z.K. and Bayomy, F.M. (1999), “Rubberized Portland cement concrete”, *J. Mater. Civil Eng*., **11**(3), 206-213.

Kim, Y.J. and Yi, C. (2015), “The UHF wave shielding effectiveness of mortar with conductive inclusions”, *J. Architec. Inst. Korea Struct. Constr.*, **31**(4), 103-110.

KSA (2014), KS C 0304 *Test method for measuring the electromagnetic shielding effectiveness of planar* Korean standards association, Korea.

Lee, S.H. and Shim, J.W. (2003), “Properties and shielding efficiency of electromagnetic wave absorbing inorganic paint using carbon”, *J. Architec. Inst. Korea Struct. Constr.*, **19**(1), 69-76.

Li, D.K. and Odouli, R. (2002), “A population-based prospective cohort study of personal exposure to magnetic fields during pregnancy and the risk of miscarriage”, *Epidemiology*, **13**(1), 9-20.

Lim, H.S. and Lee, H.S. (2011), “Experimental study on the development of X-Ray shielding concrete utilizing electronic arc furnace oxidizing slag”, *J. Architec. Inst. Korea Struct. Constr.*, **27**(7), 125-132.

Michael, P.A. (1997), *Regression analysis with standardized variables*, Springer, US.

Micheli, D. and Pastore, R. (2014), “Electromagnetic characterization and shielding effectiveness of concrete composite reinforced with carbon nanotubes in the mobile phones frequency band”, *Mater. Sci. Eng. B*, **188**, 119-129.

Min, G.C. (2009), *EMC engineering*, Jinhan MnB, Seoul

Shyr, T.W. and Shie, J.W. (2012), “Electromagnetic shielding mechanisms using soft magnetic stainless steel fiber enabled polyester textiles”, *J. Magn. Magn. Mater.*, **324**(23), 4127-4132.

Suchea, M., Tudose, I.V., Tzagkarakis, G., Kenanakis, G., Katharakis, M., Drakakis, E. and Koudoumas, E. (2015), “Nanostructured composite layers for electromagnetic shielding in the GHz frequency range”, *Appl. Surf. Sci.*, **352**, 151-154.

Wen, S. and Chung, D.D.L. (2004), “Electromagnetic interference shielding reaching 70 dB in steel fiber cement”, *Cement Concrete Res.*, **34**(2), 329-332.

White, D.R.J. and Mardiguian, M. (1988), *Electromagnetic shielding*, Interference Control Technologies.